

# Ternary Memristive Logic: Hardware for Reasoning Realized via Domain Algebra

Chao Li

Deepleap.ai lichao@deepleap.ai

## Abstract

Memristive crossbar arrays are widely used to perform matrix–vector multiplication in memory, but each junction stores only a numerical weight—a fragment whose meaning emerges only after aggregation, activation, and external decoding. A single junction, by itself, answers nothing.

This paper explores a fundamentally different use of the same hardware. Building on the CDC framework (Li, Wang & Zhao, 2026a–c), we design a system in which each memristive junction stores a complete, domain-scoped logical assertion: whether a specific relation between two concepts holds, is negated, or is undefined within a given domain. Reading one junction directly answers one question, without aggregation or interpretation.

The key contribution is not the use of ternary states, but a structure-preserving mapping from a materialized CDC domain algebra to a memristive crossbar topology. Under this mapping, domains become physically isolated arrays, specialization becomes directed inter-array wiring, relation typing controls inheritance through gated connections, and cross-domain links are realized as explicit bridge registers. In this design, the physical organization of the chip encodes the algebra itself: modifying the wiring changes the reasoning semantics.

We present a concrete implementation for ICD-11 respiratory disease classification (1,247 entities, ~136,000 junctions) using 1T1R cells. The system supports domain scoping, three-valued logic, transitive classification, typed inheritance, and cross-axis reasoning through a combination of intra-array cascades and cross-reference registers. Behavioral simulation under realistic device variability ( $\sigma_{\log} = 0.15$ , SNR = 20 dB) shows error-free operation across 100,000 trials per task, with substantial tolerance margins.

Prior work established that CDC unifies representation and computation in software. This paper demonstrates the same unification in hardware: when each stored element carries complete semantics, reasoning reduces to applying voltages and reading currents—no symbolic processing layer required.

## 1. Two Kinds of "In-Memory Computing"

### 1.1. The Neural Network Kind: Junctions as Fragments

A memristive neural network accelerator stores a weight matrix  $W$  in a crossbar array. Each junction  $(i, j)$  holds a conductance value  $G_{ij}$  representing weight  $w_{ij}$ . When a voltage vector  $V$  is applied to the input wires, the output current at wire  $j$  is:

$$I_j = \sum_i V_i G_{ij}$$

This is matrix-vector multiplication — performed in memory, with no data movement. This is genuinely valuable: it eliminates the von Neumann bottleneck for this specific operation.

**But what does junction (3, 7) mean?** It means: "the weight connecting input neuron 3 to output neuron 7 in layer k is 0.73." This is a **fragment**. By itself, it answers no question. To produce a meaningful answer — "this image is a cat" — the system must:

1. Aggregate the entire row's outputs (sum of currents)
2. Apply a nonlinear activation function (external circuit)
3. Route the result to the next layer (interconnect)
4. Repeat for every layer
5. Apply softmax and threshold (external logic)
6. Decode the output class (lookup table)

Steps 2–6 happen outside the crossbar. The crossbar computes dot products; everything else is external. **The junction stores a number. The number means nothing alone.**

### 1.2. The CDC Kind: Junctions as Complete Assertions

Now consider a different use of the same hardware. Junction (3, 7) in a specific crossbar array means:

"In the anatomical classification world, Streptococcal Pneumonia (row 3) IS\_A Pneumonia (column 7)."

And its resistance state means:

Resistance	State	Meaning
Low (conducts)	+1	Yes, this classification holds
High (blocks)	-1	No, this classification is explicitly negated
Intermediate	0	This classification is not defined in this domain

**What does reading this one junction tell you?** It tells you: in the anatomical domain, Streptococcal Pneumonia is classified as a type of Pneumonia. That is a complete clinical answer. Not a fragment. Not a partial dot product. A full, auditable, domain-scoped medical classification.

No aggregation needed. No activation function. No decoder. One junction, one read, one answer.

### 1.3. Why This Difference Matters

The difference is not about ternary vs. binary, or analog vs. digital. **The difference is whether a single junction carries complete semantics.**

In a neural crossbar, the position (i, j) tells you *where in the computation* this weight sits. In a CDC crossbar, the position tells you *what clinical fact* this junction represents. The position is the semantics.

### 1.4. The Central Claim

**When each junction in a memristive array carries complete CDC semantics — domain, relation, concepts, truth value — executing the reasoning reduces to applying voltages and reading currents, with no symbolic interpretation step in between.**

	Neural Network Junction	CDC Junction
What it stores	A numerical weight (0.73)	A logical assertion (+1 / -1 / 0)
What it means alone	Nothing (fragment of a computation)	A complete domain-scoped fact
What reading it tells you	One term of a dot product	Whether a specific relation holds in a specific domain
What else is needed for an answer	Entire network + external circuits	Nothing (or: cascade for multi-hop)
Semantic coordinates	Layer number, input index, output index (computational position)	Domain, concept, relation, target concept (semantic position)

The rest of this paper makes this precise: we establish the homomorphism between a materialized CDC domain algebra and a crossbar topology, specify the 1T1R cell and cascade circuit that realize it, introduce cross-reference registers for inter-axis bridges, and validate five reasoning capabilities by behavioral simulation.

### 1.5. Position in the CDC Series

This paper is part of a program of work on domain-contextualized reasoning. The prior papers establish the framework at progressively more operational levels:

- **Paper 1** (Li, Wang & Zhao, 2026a): establishes @D as a modal necessity operator with Kripke-style possible-world semantics. The representational claim: domain belongs in predicate arity, not metadata.
- **Paper 2** (Li, Wang & Zhao, 2026b): establishes the computable domain algebra — a Heyting algebra (their Theorem 4.9) with a typed Galois connection governing inheritance (their Theorem 4.19), and rank-1 neural convergence conditions (their Theorem 8.4).
- **Paper 3** (Li & Wang, 2026c): establishes representation-computation unity (RCU) — writing a CDC record defines its inferential behavior; reasoning is CRUD on stored four-tuples. A working Python+Prolog engine demonstrates the claim.

This paper establishes that the same representation-computation unity dissolves the storage-computation boundary in physics as well as in software. The domain algebra of Paper 2 — materialized at compile time into a specific lattice — maps onto a memristive crossbar topology; the CRUD operations of Paper 3 map onto voltage writes and current reads.

The paper claims no new algebra. Every algebraic result invoked below is from Paper 2. The contribution is the physical mapping and the circuit design that realizes it.

## 2. Background

### 2.1. Memristive Crossbar Arrays

A crossbar array is a grid of horizontal word lines and vertical bit lines, with a memristive device (variable resistor) at each intersection. Three operations:

- **Write:** Program each device to a target resistance state by applying voltage pulses.
- **Read:** Apply a voltage to a word line; measure current at each bit line. Current through junction  $(i,j) = V_i / R_{ij} = V_i \cdot G_{ij}$ .
- **Compute (in neural mode):** Apply a voltage vector to all word lines simultaneously; output current vector = conductance matrix  $\times$  voltage vector.

Passive crossbars with two-terminal memristors suffer from sneak-path currents: a voltage applied to row  $i$  and sensed on column  $j$  drives not only the target junction  $(i,j)$  but also parasitic paths through unselected junctions. For arrays beyond  $\sim 100$  junctions, this is the dominant source of read error and the reason commercial crossbar products universally adopt **1T1R cells** — a selector transistor in series with each memristor, which eliminates sneak paths by electrically isolating unselected rows (Yu et al., 2011; Chen et al., 2015). This paper assumes a 1T1R architecture throughout (Section 4.3).

### 2.2. The Precision Problem

Neural crossbars require 4–8 bit precision per junction (16–256 resistance levels) to faithfully represent continuous weight values. Achieving and maintaining this precision across millions of devices is the primary obstacle to commercialization:

- Device-to-device variability
- State drift over time
- Read noise between adjacent levels
- Programming endurance degradation

### 2.3. The CDC Framework (Summary)

Paper 1 defines a CDC four-tuple as  $\langle c, r, c', d \rangle$  where  $c, c'$  are concepts,  $r$  is a relation predicate, and  $d$  is a domain specification. An assertion  $r(c, c', d)$  takes a value in  $\{+1, 0, -1\}$ :

- **+1:**  $r(c, c')$  holds in world  $w_d$
- **-1:**  $r(c, c')$  is explicitly negated in  $w_d$
- **0:**  $r(c, c')$  is not defined in  $w_d$  (semantically irrelevant)

The third state is not "unknown" — it means the question has no answer in this domain. "Is Aspirin a drug?" is undefined in @Music. Not unknown. Meaningless.

Paper 2 establishes the domain algebra  $DA = (D, \sqsubseteq, \sqcap, \sqcup, \rightarrow, \perp, \top, \tau, F)$  where:

- $\sqsubseteq$  is the specialization order on domain strings (a partial order)
- $\sqcap$  is meet;  $\sqcup$  is join
- $\rightarrow$  is Heyting implication
- $\tau: R \rightarrow \{\text{monotone, non-monotone}\}$  is the relation typing function stored in a meta-fiber

- $F(d)$  is the fiber: the set of assertions scoped to  $d$

Paper 2 further establishes that DA is a Heyting algebra (their Theorem 4.9); that reindexing from a parent fiber to a child fiber is a  $\tau$ -typed Galois connection  $(\alpha, \gamma_\tau)$ , with  $\gamma_\tau$  undefined for non-monotone relations (their Theorem 4.19); and that monotonicity is equivalent to  $\gamma_\tau \circ \alpha$  being a closure operator (their Corollary 4.20). Paper 3 further provides cross-fiber *bridge* predicates (`same_entity_across`, `analogous_to`, `fuses_with`) that link concepts across fibers that are not in a  $\sqsubseteq$  relation.

## 2.4. Related Hardware Approaches

Several hardware paradigms store or compute logical/semantic information in memristive arrays. This paper’s contribution is distinct from each.

**Hyperdimensional Computing (HDC) / Vector Symbolic Architectures.** Kanerva (2009) and subsequent in-memory implementations (Karunaratne et al., 2020; Wu et al., 2021) encode symbols as high-dimensional bipolar vectors and perform symbolic operations through element-wise operations in memristive arrays. HDC junctions store **vector components** — a single junction is one dimension of a distributed representation, and meaning requires reading the entire vector. A CDC junction stores a **complete assertion** — meaning is localized to a single device. HDC trades localizability for noise robustness; CDC prioritizes localizability for auditability and domain scoping.

**Stateful Memristive Logic.** Borghetti et al. (2010), Kvatinsky et al. (2014), and Talati et al. (2016) use memristors as logic gates: applying voltage sequences causes resistance states to compute material-level IMPLY, NAND, or related primitives. These approaches embed **Boolean** logic in physics. CDC embeds **three-valued intuitionistic** logic with domain scoping, which stateful logic cannot natively express.

**Analog Content-Addressable Memory.** Li et al. (2020) use memristors to build analog ternary CAMs for similarity search. A TCAM performs pattern matching across a flat store; entries can be rearranged without changing semantics. In CDC, the physical layout **is** the algebra — the directed wiring topology encodes the specialization order, and rearranging the wiring changes the inference. This is the central structural difference argued in Section 3.

**Neuromorphic Chips.** IBM TrueNorth (Merolla et al., 2014), Intel Loihi 2, and BrainScaleS implement spiking neural networks. Reasoning emerges from population dynamics over many neurons. CDC reasoning is localized to individual junctions.

**Knowledge Graph Accelerators.** Recent ISCA/MICRO work builds specialized hardware for embedding-based KG completion. These accelerate matrix operations on pre-trained embeddings; they do not store symbolic assertions directly.

In this design space, CDC occupies a previously unfilled position: **localized, symbolic, three-valued, domain-scoped, auditable.**

## 3. From Algebra to Physics: The Structural Homomorphism

We now present the mapping  $\Phi$  formally. Readers unfamiliar with the CDC algebra may interpret it operationally as a compile-time embedding of domain structure into crossbar topology: domains become arrays, inheritance becomes wiring, and relation typing controls current flow. The formal statements below make this correspondence precise.

The central contribution of this paper is that the Heyting algebra of Paper 2, once materialized at compile time into a specific domain lattice, maps structure-preservingly onto a memristive crossbar

topology. We stress that Paper 2 has already done the algebraic work — the results we need are already proved there. This section defines the materialized algebra  $DA^*$ , the crossbar topology CT, the map  $\Phi: DA^* \rightarrow CT$ , and shows that  $\Phi$  preserves each algebraic property.

### 3.1. Compile-Time Materialization

The domain algebra DA defined in Paper 2 is a general algebraic framework; any specific application instantiates it with a concrete set of domains, a concrete specialization order, a concrete set of bridges, and a concrete typing function. We call this instantiation a **materialized domain algebra**, denoted  $DA^*$ .

The hardware presented here realizes a **single materialized snapshot** of  $DA^*$ . At compile time, the domain lattice is crystallized into directed wiring between arrays; the typing function is crystallized into the state of a meta-array; cross-fiber bridges are crystallized into cross-reference registers. Once the chip is fabricated, this structure is fixed: the memristive states within each array remain programmable (supporting INSERT, UPDATE, DELETE of individual assertions), but the inter-array topology does not.

Runtime evolution of the domain lattice itself — for example, through mechanisms that split a domain when a new assertion creates a contradiction — is handled in software and falls outside the scope of this physical implementation. Such mechanisms produce a new  $DA^*$ , which can be compiled to a new chip or loaded onto a reconfigurable platform; neither extension is pursued here.

This framing has two consequences for what follows. First, we do not need to commit to whether the specialization order in  $DA^*$  is a tree, a DAG with multiple inheritance, or some other partial order shape: whatever partial order the compiler hands us, we materialize it as directed wiring. Second, concepts that participate in multiple classification axes simultaneously — for example, a disease that belongs to an anatomical classification, an etiological classification, and a clinical classification at the same time — are handled not by making one domain the child of multiple parents, but by treating each classification axis as its own domain tree and linking concepts across axes through bridges. This is exactly how Paper 3 §9 represents ICD-11 multi-axis classification: via `same_entity_across` bridges, not via multi-parent  $\sqsubseteq$  edges.

### 3.2. The Physical Structure: Crossbar Topology

Define the physical structure of a memristive crossbar system as:

$$CT = (A, \sqsubseteq_A, W, G, S, M, B)$$

### 3.3. The Mapping $\Phi: DA^* \rightarrow CT$

$\Phi$  is a family of six sub-mappings that jointly act on the carriers and operations of  $DA^*$ . Informally,  $\Phi$  takes every algebraic component of  $DA^*$  and returns its physical counterpart in CT; formally, it is the ordered collection  $(\Phi_D, \Phi_F, \Phi_S, \Phi_{\sqsubseteq}, \Phi_{\tau}, \Phi_B)$ :

**Note on  $\Phi_{\tau}$ .** In Paper 3,  $\tau$  is stored as a small number of four-tuples of the form `{from: r, rel: has_property, domain: @Meta@Logic, to: monotone/non_monotone}` — one entry per relation  $r$ , independent of any specific domain pair. Physically, however, each parent-child inheritance edge that involves relation  $r$  needs its own gate transistor, so  $\Phi_{\tau}$  does not simply copy  $\tau$ : it *unfolds*  $\tau$  across the inheritance edge set. For each triple  $(r, d_p, d_c)$  where  $d_c \sqsubseteq d_p$ ,  $\Phi_{\tau}$  produces a gate  $G(r, d_p, d_c)$  whose state is determined by  $\tau(r)$ . The meta-array M stores one ternary junction per relation type (the underlying  $\tau$ ), and a **CMOS buffer tree** amplifies and replicates each meta-junction’s state to all gate transistors associated with that relation. The buffer tree is necessary because a

Symbol	Meaning	Physical realization
A	Set of crossbar arrays	Physically separate array regions on chip
$\sqsubseteq_A$	Connection ordering between arrays	Directed wiring: array $a_1$ can send current to $a_2$
W	Set of junctions across all arrays	1T1R cells at crossbar intersections
G	Gate states on inter-array connections	Transistor switches between arrays: ON/OFF
S: $W \rightarrow \{+1, 0, -1\}$	State function: each junction's resistance	$R_{\text{low}} / R_{\text{mid}} / R_{\text{high}}$
M	Meta-array storing $\tau$	Small crossbar whose junction states drive G
B	Cross-reference register bank	Registers linking concepts across non-comparable domains

Domain Algebra (DA*)	Sub-mapping	Crossbar Topology (CT)
Domain $d \in D$	$\Phi_D$	Array $a_d \in A$
Fiber $F(d)$	$\Phi_F$	Junction states in array $a_d$
Assertion state $\{+1, 0, -1\}$	$\Phi_S$	$R_{\text{low}} / R_{\text{mid}} / R_{\text{high}}$
Specialization $d_c \sqsubseteq d_p$	$\Phi_{\sqsubseteq}$	Directed wire from $a_{d_p}$ to $a_{d_c}$
Typing $\tau$ , unfolded over inheritance edges	$\Phi_{\tau}$	Meta-array states driving gate transistors G
Bridge predicate $\text{bridge}(c, c', d_1, d_2)$	$\Phi_B$	Entry in cross-reference register bank B

single memristive junction cannot directly drive thousands of transistor gates — its current output is orders of magnitude below the required fan-out. The tree is a standard logarithmic-depth driver fabric (typical fan-out of 4 per stage,  $\sim 6$  stages to reach 8K gates), contributing negligible area and  $\sim 1$  ns propagation delay to the gate-update path. For the ICD-11 chip of Section 4, this yields 8 meta-junctions driving  $\sim 8,600$  gate transistors through  $\sim 60$  buffer stages in total (distributed across relation types).

**Note on  $\Phi_B$ .** Bridges in Paper 3 link concepts across fibers that are **not in a  $\sqsubseteq$  relation** — for example, viral pneumonia's identity across the anatomical and etiological classification axes. Because these links do not flow along the specialization order, they cannot be implemented by directed inter-array wiring; instead, we implement them as explicit cross-reference registers (Section 4.4).  $\Phi_B$  is therefore a separate mapping channel from  $\Phi_{\sqsubseteq}$ , and this separation is essential: collapsing bridges into  $\sqsubseteq$  edges would corrupt the algebra.

### 3.4. Seven Lemmas: $\Phi$ Preserves the Domain Algebra

We now state seven lemmas. Each is of the form "Paper 2 (or Paper 3, for bridges) establishes algebraic property X;  $\Phi$  preserves X." Together they constitute Theorem 1.

Algebraic state	Physical state	Electrical behavior
+1 (holds)	$R_{\text{low}}$ (~10 k $\Omega$ )	High current — conducts
0 (undefined)	$R_{\text{mid}}$ (~100 k $\Omega$ )	Intermediate current
-1 (negated)	$R_{\text{high}}$ (~1 M $\Omega$ )	Near-zero current — blocks

**Lemma 3.4.1 (Fiber isolation).** By Paper 2 Definition 3.3,  $F(d_1) \cap F(d_2) = \emptyset$  for  $d_1 \neq d_2$ . Under  $\Phi$ , arrays  $a_{\_}\{d_1\}$  and  $a_{\_}\{d_2\}$  are physically separate — non-overlapping regions with no shared word or bit lines. *Proof:*  $\Phi_D$  maps distinct domains to distinct arrays;  $\Phi_F$  maps disjoint fibers to junctions in disjoint arrays. Current applied to  $a_{\_}\{d_1\}$  cannot produce current in  $a_{\_}\{d_2\}$  without traversing either a gated inter-array connection ( $\Phi_{\sqsubseteq}$ ) or a cross-reference register access ( $\Phi_B$ ). Both are explicit operations; neither is a leakage path.  $\square$

**Lemma 3.4.2 (Ternary valuation).** By Paper 2 Section 4.1, each assertion in  $F(d)$  takes a value in  $\{+1, 0, -1\}$ . Under  $\Phi_S$ , these map bijectively to  $\{R_{\text{low}}, R_{\text{mid}}, R_{\text{high}}\}$ .

*Proof:* A two-threshold comparator ( $I_{\text{high}} > I_{\text{mid}} > I_{\text{low}}$ ) distinguishes all three states.  $\square$

*Why ternary, not binary:* "Aspirin is contraindicated in pediatrics" (-1) requires active warning; "Aspirin has no established role in veterinary medicine" (0) requires no action. Binary encoding collapses both into "not true" and loses this safety-critical distinction.

**Lemma 3.4.3 (Specialization order).** By Paper 2 Definition 4.2,  $\sqsubseteq$  is a partial order on domain strings. Under  $\Phi_{\sqsubseteq}$ , for each pair  $(d_c, d_p)$  in  $DA^*$  with  $d_c \sqsubseteq d_p$ , there is a directed wire from  $a_{d_p}$  to  $a_{d_c}$ . Incomparable domains are physically unconnected. *Proof:* the partial order of  $DA^*$  is given at compile time.  $\Phi_{\sqsubseteq}$  instantiates it as a directed inter-array graph: every covering pair in the Hasse diagram of  $(D, \sqsubseteq)$  becomes a physical wire; reachability in the array graph matches reachability in the order. The shape of the partial order — tree, DAG, or otherwise — is determined by  $DA^*$  and reproduced verbatim by  $\Phi_{\sqsubseteq}$ ; the physical mechanism is indifferent to this shape, as long as the fan-in at each array is within the driver's capacity.  $\square$

**Lemma 3.4.4 (Meet).** By Paper 2 Definition 4.4,  $d_1 \sqcap d_2$  is the longest common prefix (the greatest lower bound under  $\sqsubseteq$ ). Under  $\Phi$ , this corresponds to the greatest common ancestor in the directed array graph. *Proof:* By Lemma 3.4.3, the array graph mirrors  $(D, \sqsubseteq)$ . The meet is the greatest lower bound of two elements in the partial order; under the physical graph, this is computable by intersecting the downward-closures of  $a_{\_}\{d_1\}$  and  $a_{\_}\{d_2\}$  and selecting the maximum — implementable as a short circuit trace.  $\square$

**Lemma 3.4.5 (Heyting implication).** By Paper 2 Theorem 4.9,  $d_1 \rightarrow d_2 = \sqcup_{\_}\Delta \{d \mid d \sqcap d_1 \sqsubseteq d_2\}$ . Under  $\Phi$ , this is the least upper bound of all arrays  $a_d$  such that any path from  $a_d$  passing through  $a_{\_}\{d_1\}$  also reaches  $a_{\_}\{d_2\}$ . *Proof:* By Lemmas 3.4.3 and 3.4.4,  $\sqsubseteq$  and  $\sqcap$  are preserved as reachability and common-ancestor operations on the array graph. The Heyting implication is the join of a downward-closed set; Paper 2 Lemma 4.7 (Prefix Distributivity) ensures this join is well-defined. Computationally, the implication is determined by a backward reachability trace: starting from  $a_{\_}\{d_2\}$ , walk backward along  $\sqsubseteq_A$  edges to find arrays whose every path through  $a_{\_}\{d_1\}$  terminates in  $a_{\_}\{d_2\}$ . This is  $O(|A|)$  in the number of arrays.  $\square$

**Lemma 3.4.6 (Typed Galois connection).** By Paper 2 Theorem 4.19,  $(\alpha, \gamma_{\tau})$  is a Galois connection on the monotone subcategory of relations, with  $\gamma_{\tau}$  undefined on the non-monotone subcategory. Under  $\Phi_{\tau}$ , for each inheritance edge  $(d_c \sqsubseteq d_p)$  and each relation  $r$ , the gate  $G(r, d_p, d_c)$  is driven by the meta-junction encoding  $\tau(r)$ :

- $\tau(r) = \text{monotone} \rightarrow \text{meta-junction at } R_{\text{low}} \rightarrow \text{gate driver output HIGH} \rightarrow G(r, d_p, d_c) \text{ ON} \rightarrow$  current can flow from  $a_{d_p}$  to  $a_{d_c}$  for relation  $r$ . Physically:  $\gamma_\tau$  is defined on this edge for this relation; an inherited assertion exists in the child fiber.
- $\tau(r) = \text{non-monotone} \rightarrow \text{meta-junction at } R_{\text{high}} \rightarrow \text{gate driver output LOW} \rightarrow G(r, d_p, d_c) \text{ OFF} \rightarrow$  no current path exists. Physically:  $\gamma_\tau$  is undefined on this edge for this relation; the assertion cannot be inherited.

*Proof:* The gate does not filter inherited assertions — it enables or disables the electrical path. When  $G(r, d_p, d_c)$  is OFF, no current path exists for relation  $r$  on that edge. This is the physical realization of "undefined" in the typed Galois connection: not "checked and rejected," but "structurally impossible." Because  $\Phi_\tau$  unfolds a single  $\tau(r)$  value to all gates  $G(r, \cdot, \cdot)$  for that relation (Section 3.3), a single meta-junction state simultaneously governs all inheritance edges for  $r$ .  $\square$

*Why this is the decisive distinction from TCAM:* In a TCAM, all entries are equally accessible; preventing inheritance requires a software rule that can be bypassed, misconfigured, or forgotten. In CT,  $G(r, d_p, d_c)$  is a physical switch. When OFF, no software can make the current flow through it. The constraint is not in code — it is in physics.

**Lemma 3.4.7 (Closure property).** By Paper 2 Corollary 4.20,  $\gamma_\tau \circ \alpha$  is a closure operator on monotone relations:  $(\gamma_\tau \circ \alpha) \circ (\gamma_\tau \circ \alpha) = \gamma_\tau \circ \alpha$ . Under  $\Phi$ , this is physical write-idempotence: after reindexing has populated  $a_{d_c}$  with inherited junctions from  $a_{d_p}$ , re-running the inheritance cycle writes the same junction states. *Proof:* Re-inheritance attempts to write values identical to those already present. RRAM and PCM devices tolerate redundant writes to the same target state with negligible state change (Wong & Salahuddin, 2015); the circuit is naturally idempotent at the device level.  $\square$

**Lemma 3.4.8 (Bridge preservation).** By Paper 3 Section 9, bridge predicates such as `same_entity_across`, `analogous_to`, and `fuses_with` link concepts across fibers whose domains are not in a  $\sqsubseteq$  relation. Under  $\Phi_B$ , each bridge predicate instance is stored as an entry in the cross-reference register bank  $B$ . Read access to a bridge entry returns the target concept and domain without traversing  $\sqsubseteq_A$  wiring.

*Proof:*  $\Phi_B$  maps bridge four-tuples in  $DA^*$  to register entries in  $B$ . A bridge from  $(c, d_1)$  to  $(c', d_2)$  with incomparable domains is stored as a register entry indexed by  $(c, d_1)$  and returning  $(c', d_2)$ . Reading the register is a constant-time operation orthogonal to  $\sqsubseteq_A$  wiring; the bridge does not flow along the specialization order and therefore does not interact with the Galois connection or the inheritance gates.  $\square$

### 3.5. Theorem 1

**Theorem 1 (Structural homomorphism).**  $\Phi: DA^* \rightarrow CT$  preserves the full algebraic structure of the materialized CDC domain algebra: fiber isolation, ternary valuation, specialization order, meet, Heyting implication, typed Galois connection, closure property, and bridges.

*Proof:* By Lemmas 3.4.1 through 3.4.8.  $\square$

### 3.6. Why This Is Not TCAM: A Summary

**A TCAM stores values. CT stores an algebra.**

### 3.7. Five Reasoning Functions as Consequences

The lemmas yield five reasoning capabilities as direct consequences:

Property	TCAM	CDC Crossbar Topology (CT)
Physical layout	Flat: all entries in one array	Structured: arrays connected by directed wiring + bridges
Layout carries meaning	No: entries can be rearranged arbitrarily	Yes: wiring topology = domain lattice
Domain scoping	Software filter on match fields	Physical array isolation
Specialization order	Not represented in hardware	Directed inter-array connections
Meet ( $\sqcap$ )	Not computable from hardware	Circuit trace: most specific common ancestor
Heyting implication ( $\rightarrow$ )	Not representable	Backward reachability on array graph
Typed inheritance	Software rule (bypassable)	Physical gate $G(r, d_p, d_c)$ (not bypassable)
Cross-fiber bridges	Not representable	Cross-reference register bank
Closure property	Not applicable	Re-running inheritance = no change

**Consequence 1: Domain scoping** follows from Lemma 3.4.1 — current in one array cannot leak to another without an explicit gated or register-mediated path.

**Consequence 2: Three-valued logic** follows from Lemma 3.4.2 — each junction’s physical state IS its logical state.

**Consequence 3: Transitive classification** follows from Lemma 3.4.1 + 3.4.2 — within an isolated array, the cascade mechanism (Section 4.3) computes transitive closure by iterating row-input/column-output cycles.

**Consequence 4: Typed knowledge inheritance** follows from Lemma 3.4.3 + 3.4.6 — specialization order as directed wiring, Galois connection as meta-gated paths  $G(r, d_p, d_c)$ .

**Consequence 5: Intra-array write-time consistency checking** follows from Lemma 3.4.1 + 3.4.2 — because all explicitly stored assertions in a domain coexist in the same physical array, checking for immediate contradictions before writing is a single READ cycle on the same array. The validator IS the knowledge base. *Transitive consistency across inherited assertions in other domains requires a full cascade check and is handled at a higher layer of the write controller.*

**Cross-axis queries**, where two or more incomparable domains are consulted in the same inference, are handled by Consequence 4 within each domain tree followed by  $\Phi_B$  register lookups across trees (Section 4.4).

### 3.8. CRUD Operations as Voltage/Current Operations

Paper 3 Corollary 4 established that database operations on CDC four-tuples are simultaneously inference operations. Under  $\Phi$ , those database operations become voltage and current operations:

Paper 3 dissolved the storage-computation separation in software. The same dissolution holds in hardware under  $\Phi$ .

Database (Paper 3)	Inference (Paper 3)	Hardware (this paper)
INSERT {c, r, d, c'}	Assert domain-scoped fact	SET pulse at junction (c, r, c') in $a_d$
SELECT WHERE domain=d	Query within a world	Voltage on row c in $a_d$ , sense current on column c'
DELETE {c, r, d, c'}	Retract belief	Partial-RESET to $R_{mid}$ at that junction
JOIN on domain	Transitive inference	Cascade read within $a_d$ (Section 4.3)
FOREIGN KEY to meta-fiber	Enforce type constraint	Meta-array state driving $G(r, d_p, d_c)$
Bridge lookup	Cross-fiber reference	Cross-reference register read

## 4. Putting It Together: The ICD-11 Reasoning Chip

### 4.1. What We Are Building

A chip that performs domain-scoped medical classification for ICD-11 respiratory diseases. Given a disease entity and a classification axis, the chip returns the complete classification chain in hardware. Following Paper 3 §9, we treat ICD-11's three classification axes — Anatomical, Etiological, Clinical — as **three parallel domain trees** rather than as multiple inheritance within one tree. Entities that belong in all three (e.g., Viral Pneumonia) are linked across trees by `same_entity_across` bridges. This matches the representational choice made in Paper 3 for the same data.

## 4.2. Physical Layout

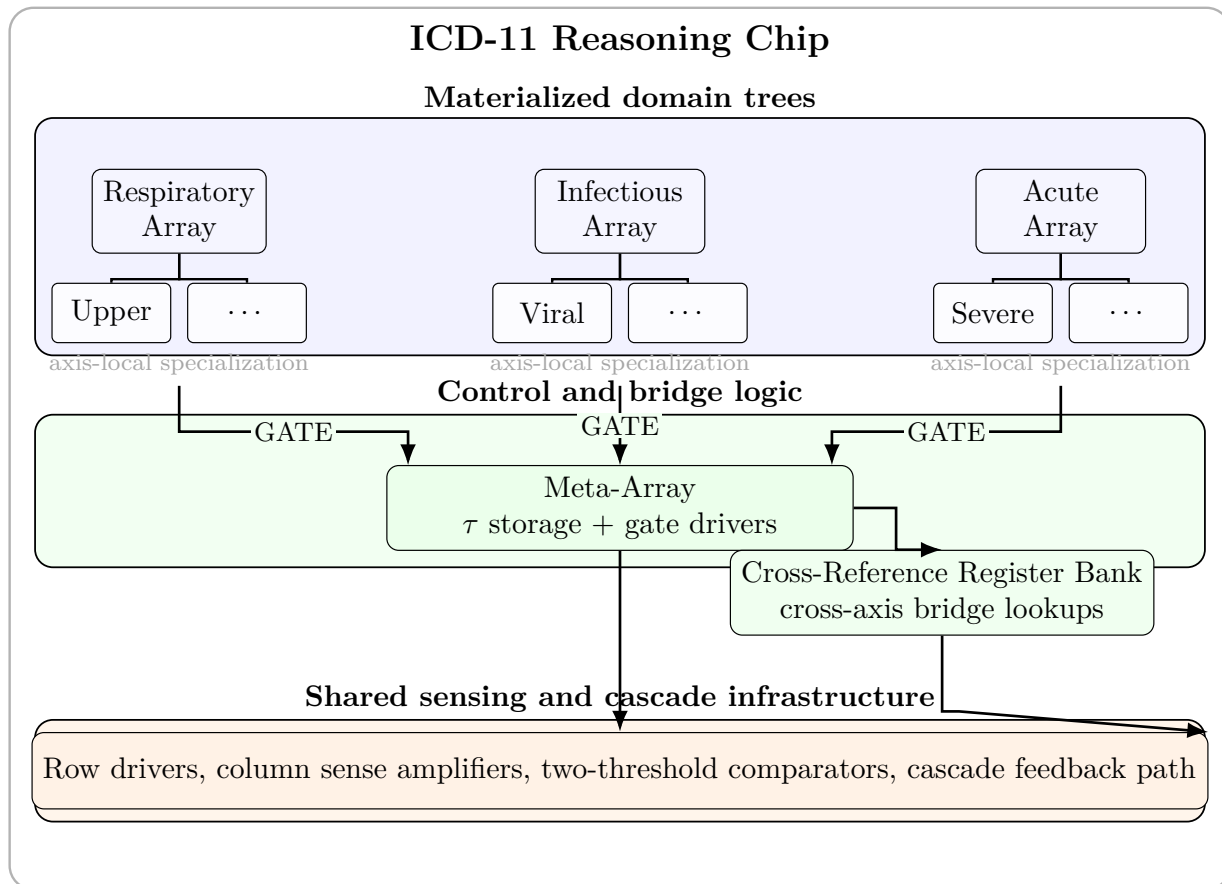


**Figure 1:** Publication-style layout of the ICD-11 reasoning chip. The top band shows three materialized domain trees as isolated crossbar families; arrows run consistently downward into the meta-array that governs typed inheritance; cross-axis queries are handled by a dedicated bridge-register bank; and the bottom band groups the shared sensing and cascade circuitry.

## 4.3. The Cascade Mechanism

Consequence 3 (transitive classification) requires cascading reads within an array. We now specify the circuit that implements this process and analyze its complexity.

Each domain array is organized as a **square** crossbar indexed by concept: the same concept appears as both a row (source) and a column (target). A single read cycle applies a voltage to one row and senses currents on all columns. For transitive closure, the column currents where output = +1 must be re-driven as row voltages in the next cycle. The cascade circuit implements the following sequence:

**Why only one row is activated per cycle.** Activating two rows simultaneously would superpose their column-current signatures, and the two-threshold comparator could not distinguish "row A triggered this column at +1" from "row B triggered this column at +1, row C at -1, net +1." The circuit serializes the cascade frontier to preserve per-junction resolution.

**Why 0 and -1 states do not propagate.** The intermediate current of the 0 state ( $R_{\text{mid}}$ ,  $\sim 2 \mu\text{A}$ ) and the near-zero current of the -1 state ( $R_{\text{high}}$ ,  $\sim 0.2 \mu\text{A}$ ) both fall below the positive-threshold

Step	Operation
Cycle 1	Apply the row driver to concept CA40.00; column sense amplifiers read the resulting current vector.
Thresholding	Two-threshold comparators convert the analog readout into a ternary state vector $T_1 \in \{+1, 0, -1\}^N$ .
Latch state	Store the positive frontier as $S_1 = \{c' : T_1[c'] = +1\}$ .
Cycle $k+1$	Pick the next unvisited concept $c \in S_k$ , drive its row, sense all columns, and append new positive outputs to $S_{k+1}$ .
Stop rule	Terminate when a cycle yields no new +1 outputs, indicating that the root has been reached.

**Table 1:** Cascade-read procedure used for transitive classification within a single domain array.

comparator ( $I_{\text{high}} = 6.32 \mu\text{A}$ ). They therefore cannot enter the latch and cannot be chosen as next-cycle row activations. Undefined and negated semantic paths are pruned from the cascade frontier purely by physical current thresholds, with no conditional-branching logic, no software filter, and no extra cycles. **What takes a query optimizer a pass to compute in software is an inherent property of the circuit.** This is a structural benefit of embedding three-valued logic in physics rather than layering it on top of binary computation.

**Why the total cycle count stays bounded.** The apparent worst case "N concepts  $\times$  4 steps = 4N reads" does not occur because the cascade frontier does not fan out linearly: `is_a` is a tree, and a disease classifies into  $O(d)$  ancestors where  $d$  is the depth of the taxonomy (typically 4–6 for ICD-11). The actual cycle count is  $O(d)$ , not  $O(N)$ .

**Why threshold regeneration matters.** The cascade is not continuous analog current flow — it is a sequence of discrete, digitized reads. Continuous analog propagation would accumulate read noise across cycles and collapse the three-state distinction after 2–3 hops. Each discrete read is threshold-restored to  $\{+1, 0, -1\}$ , preventing noise accumulation. This is the same principle as regenerative digital logic.

**Why 1T1R is required.** In a passive crossbar, applying voltage to a row drives current through every junction on that row including junctions in  $R_{\text{mid}}$ , producing a sneak-current background that can exceed the target signal for realistic array sizes. The 1T1R selector transistor ensures that only the explicitly addressed cell is active in a column, and only junctions in  $R_{\text{low}}$  contribute to that column’s sensed current.

**Timing breakdown (nominal, per cascade cycle within one axis):**

Meta-array updates ( $\tau$  writes) and bridge-register accesses run on separate paths and do not add to the cascade critical path. A  $\tau$  update, when needed, incurs one meta-junction write plus a  $\sim 1$  ns buffer-tree propagation delay (§3.3) before the new gate pattern is stable — orders of magnitude below the minutes-to-yearly timescale of knowledge-base updates.

A 4-step classification cascade within one axis:  $\sim 40$  ns. Full ICD-11 query across 3 axes plus cross-axis bridge lookups:  $\sim 120$  ns. For comparison, the Paper 3 software engine on commodity hardware takes  $< 20$  ms for the same query — a  $\sim 5$  order-of-magnitude reduction, driven not by clever optimization but by the absence of a software stack.

Stage	Time	Notes
Row driver rise (word-line charge)	1 ns	Standard CMOS driver
Word line + access-transistor settle	2 ns	1T1R access delay
Column sense-amp integration	5 ns	Dominant term; current mirror + capacitor integration
Two-threshold comparator	1 ns	Paired latched comparators
Latch + control sequencer	1 ns	Cascade-frontier update
<b>Per-cycle total</b>	<b>~10 ns</b>	

#### 4.4. Cross-Reference Registers

Bridges link concepts across axes. For ICD-11, the dominant bridge is `same_entity_across` — e.g., CA40.00 (Streptococcal Pneumonia) as the "same entity" in the Anatomical, Etiological, and Clinical axes. We implement the register bank as follows:

- **Indexed by** (`concept_id`, `axis_id`): a 16-bit concept address plus a 2-bit axis tag
- **Returns** a list of (`concept_id`, `axis_id`) pairs, one per axis where the same entity appears
- **Size** for the respiratory chapter: ~3,000 entries (roughly one-third of concepts participate in cross-axis bridges), 8 bytes per entry, ~24 KB total — a negligible silicon footprint

Bridge reads occur in parallel with axis cascade reads, adding no latency to the critical path. A full cross-axis query executes as: cascade within each axis, then read bridge registers to align the three result chains at the entity level.

This register bank is the physical realization of  $\Phi_B$  (Lemma 3.4.8). It is deliberately kept structurally separate from the  $\sqsubseteq_A$  wiring: bridges are not inheritance and must not be treated as such.

## 4.5. Specifications

Parameter	Value	Note
Classification axes	3	Anatomical, Etiological, Clinical
Arrays per axis (avg)	~16	Taxonomic subdomains within each axis
Total arrays	47	Across all three axes
Junctions per array (avg)	~2,900 (61×48)	Concepts × relations in that domain
Cell structure	1T1R	Selector transistor in series with memristor
Total memristive junctions	~136,000	All domain arrays combined
Meta-crossbar junctions	8	8 relation types in @Meta@Logic ( $\tau$ only depends on $r$ )
Inter-array gate transistors	~8,600	$\tau$ unfolded across all inheritance edges
Cross-reference register entries	~3,000	Bridges between axes
Resistance states per junction	3	$\{R_{low}, R_{mid}, R_{high}\}$
Precision required	1.58 bits	$\log_2(3)$ — vs. 4–8 bits for neural
Read circuit	Two-threshold comparator	vs. precision ADC for neural

## 4.6. Example: Full Diagnostic Query

**Clinical question:** "Classify CA40.00 (Streptococcal Pneumonia) across all axes."

### Hardware operation:

STEP 1: Select @Anatomical axis. Apply voltage at CA40.00 row of the leaf array.

-> Cycle 1: +1 at "Pneumonia" column

-> Cycle 2: Pneumonia -> +1 at "Lower\_Resp\_Infection"

-> Cycle 3: Lower\_Resp\_Infection -> "Respiratory\_Disease"

-> Cycle 4: no new +1 outputs (STOP)

RESULT: CA40.00 is a Respiratory Disease (anatomical axis), 4 cycles

STEP 2: Read cross-reference register for (CA40.00, Anatomical).

$\$ \backslash \text{to} \$$  Returns: (CA40.00, Etiological), (CA40.00, Clinical)

(The "same entity" appears in all three axes at these addresses.)

STEP 3: Select @Etiological axis. Apply voltage at CA40.00 row.

$\$ \backslash \text{to} \$$  Cascade: Bacterial\_Infection  $\$ \backslash \text{to} \$$  Infectious\_Disease  $\$ \backslash \text{to} \$$  STOP

RESULT: CA40.00 is an Infectious Disease (etiological axis), 3 cycles

```
STEP 4: Select @Clinical axis. Apply voltage at CA40.00 row.  
$\\to$ Cascade: Acute_Lower_Respiratory $\\to$ STOP  
RESULT: CA40.00 is Acute Lower Respiratory (clinical axis), 2 cycles
```

Total: 9 cascade cycles + 1 register read  $\approx 90$  ns + 1 ns  $\approx 91$  ns.

Note that the bridge register in STEP 2 is read once and used to index into both subsequent axes — without bridges, STEP 3 and STEP 4 would need to re-derive CA40.00’s identity in the other axes from its classification, which is not in general possible.

## 5. Fabrication Feasibility and Behavioral Validation

### 5.1. Three-State Memristors: A Solved Problem

Unlike neural accelerators that demand 4–8 bit precision (16–256 resistance levels), CDC reasoning requires only three states. Three-state memristive operation has been demonstrated in multiple material systems:

- **HfO<sub>2</sub>-based RRAM:** SET (low R), RESET (high R), and partial-SET (intermediate R) are well-characterized states with resistance ratios  $>10\times$  between adjacent levels.
- **Phase-change memory:** Amorphous (high R), partial crystalline (mid R), and full crystalline (low R) provide three thermodynamically distinct states.

The fabrication advantage is substantial: three widely-spaced levels tolerate much higher device variability than multi-level programming. The yield and reliability requirements are dramatically relaxed.

### 5.2. Scale

136,000 memristive junctions plus  $\sim 8,600$  selector transistors and  $\sim 8,600$  gate transistors for the respiratory chapter. The full ICD-11 ( $\sim 85,000$  entities,  $\sim 500$  domains) would require approximately 7–10 million junctions — well within demonstrated crossbar capacities (Yao et al., 2020 demonstrated 2M+ junctions in a single wafer-scale design).

### 5.3. What Is Needed from a Fabrication Partner

1. A 1T1R memristive crossbar programmable to 3 stable resistance states (HfO<sub>2</sub> RRAM or equivalent), with  $\geq 10\times$  resistance ratio between adjacent levels
2. CMOS-memristor BEOL integration at a conventional logic node (28 nm and below is standard for RRAM demonstrations)
3. Transistor-gated inter-array connections — access transistors driven by a CMOS buffer tree from the meta-array
4. Two-threshold current-mode sense amplifiers (paired latched comparators, substantially simpler than the  $\geq 8$ -bit ADCs required for analog neural inference)
5. Row/column drivers and a cascade-feedback controller (standard digital CMOS)
6. A modest SRAM register bank for cross-axis bridges ( $\sim 24$  KB for the respiratory chapter)
7. Total 1T1R cell count:  $\sim 136,000$  for the proof-of-concept respiratory chapter

This is a modest fabrication target for any lab with operational 1T1R crossbar capability.

Test	Query	Expected	Observed
C1 (scope)	Read within isolated array; check no column leakage to unrelated fiber	Zero cross-array current	0 errors / 400,000 reads
C2 (ternary)	Per-state read fidelity for each of $\{+1, 0, -1\}$	Correct decode	0 errors / 300,000 reads
C3 (cascade)	4-step classification CA40.00 $\rightarrow$ Pneumonia $\rightarrow$ Lower_Resp $\rightarrow$ Respiratory_Disease	Correct chain	0 errors / 100,000 runs
C4 (inheritance)	Meta-gate decodes $\tau(r)$ under read noise	ON for monotone, OFF for non-monotone	0 errors / 200,000 trials
C5 (write check)	Read-before-write detects same-pair contradiction	Reject write	0 errors / 100,000 trials
C6 (bridge)	Cross-reference register lookup	Deterministic	0 errors / 300,000 lookups

#### 5.4. Behavioral Simulation

To validate that all six reasoning capabilities function correctly under realistic device non-idealities, we implemented a Python + NumPy behavioral model of the full system. The code and raw output are released with the paper.

##### Model parameters.

- Three resistance states with  $10\times$  spacing:  $R_{\text{low}} = 10 \text{ k}\Omega$  (+1),  $R_{\text{mid}} = 100 \text{ k}\Omega$  (0),  $R_{\text{high}} = 1 \text{ M}\Omega$  (-1)
- Read voltage  $V_{\text{read}} = 0.2 \text{ V}$ , giving nominal currents of 20, 2, and  $0.2 \mu\text{A}$  respectively
- Device variability: log-normal resistance distribution with  $\sigma_{\log} = 0.15$  (15% on log scale, matching commercial HfO<sub>2</sub> RRAM characterization)
- Read noise: additive Gaussian on sense current, SNR = 20 dB (noise\_std = signal / 10)
- 1T1R selector: ideal switch; sneak paths eliminated by construction
- Two-threshold comparator at geometric-mean thresholds:  $I_{\text{high}} = 6.32 \mu\text{A}$ ,  $I_{\text{low}} = 0.632 \mu\text{A}$

##### Test suite at nominal operating point (100,000 trials per test).

**All six tests pass at 100% under 100,000 trials.** The empirical upper bound on the failure rate at the nominal operating point is therefore  $<10^{-5}$ ; theoretical analysis (three states separated by  $\geq 5\sigma$  margin at  $\sigma_{\log} = 0.15$ ) predicts the true rate is  $\sim 10^{-10}$  or lower.

##### Safety margin (variability sweep).

To characterize the design envelope, we swept  $\sigma_{\log}$  from 0.10 to 0.50 holding SNR = 20 dB constant (simulation figure omitted). The per-state and cascade error rates are:

Three findings are worth noting.

$\sigma_{\log}$	+1 error	0 error	-1 error	4-step cascade
0.15 (nominal)	$<10^{-5}$	$<10^{-5}$	$<10^{-5}$	$<10^{-5}$
0.20	$<10^{-5}$	$<10^{-5}$	$<10^{-5}$	$<10^{-5}$
0.25	0.001%	0.006%	0.001%	0.002%
0.30	0.011%	0.022%	0.014%	0.049%
0.35	0.080%	0.154%	0.072%	0.229%
0.40	0.270%	0.529%	0.226%	0.770%
0.50	1.244%	2.390%	1.163%	3.560%

First, the design tolerates variability up to  $\sigma_{\log} \approx 0.25$  with no observable errors — a 67% headroom over the nominal value. Commercial HfO<sub>2</sub> RRAM typically achieves  $\sigma_{\log} \approx 0.10$ – $0.20$ , placing the design comfortably inside the safe region.

Second, the "0" (undefined) state is approximately twice as error-prone as  $\pm 1$  at any given variability. This is a structural property of any ternary encoding: the middle state is vulnerable to noise excursions in both directions, whereas the extreme states are vulnerable only in one. It is not a flaw of the design — it is a property of three-valued readout under Gaussian noise — but it justifies designing the undefined state to be the **safe default**: an assertion drifting from +1 or -1 toward 0 becomes "unanswerable," which a clinical controller can flag for refresh, rather than silently flipping to the opposite truth value.

Third, cascade errors scale roughly as  $2$ – $3\times$  the single-junction error rate over a 4-step cascade, not exponentially. This is the benefit of threshold regeneration (Section 4.3): each cycle restores the signal to a clean ternary state before feeding the next. Without regeneration, analog accumulation over 4 steps would amplify errors by a factor of  $\sigma \times \sqrt{4} = 2\sigma$  on each side — an exponentially degrading margin. With regeneration, the compounding is linear in cycle count rather than multiplicative.

**What the simulation does not cover.** The simulation is behavioral, not circuit-level. It does not model transistor dynamics (the 10 ns cycle estimate is a timing budget, not a SPICE result), long-term resistance drift (months to years), write endurance ( $10^6$ – $10^9$  cycles for RRAM, not a concern for yearly-update knowledge bases), or full-chapter integration beyond the respiratory subset. These are acknowledged as open items for tape-out validation (§7.4).

*Simulation figure omitted: Error rate vs. device variability at SNR = 20 dB. Left: per-state single-junction error. Right: 4-step cascade error. Dashed line marks the nominal operating point.*

## 6. Comparison: CDC Chip vs. Neural Accelerator for Medical Reasoning

### 7. Discussion

#### 7.1. What Is New Here

Not ternary computing (Knuth, 1959; Soviet Setun, 1958). Not in-memory computing (Hu et al., 2018). Not memristive logic (Borghetti et al., 2010). Not TCAM (Pagiamtzis & Sheikholeslami, 2006). Not hyperdimensional in-memory computing (Karunaratne et al., 2020). What is new:

**A structural homomorphism between a materialized CDC domain algebra and a crossbar topology, with an explicit treatment of bridges.** Prior memristive computing maps

Aspect	Neural Memristive Accelerator	CDC Reasoning Chip
<b>What one junction means</b>	A weight (fragment, no meaning alone)	A clinical assertion (complete, self-contained)
<b>Reading one junction gives you</b>	One term of a dot product	One clinical answer
<b>Domain scoping</b>	Impossible at hardware level	Physical array isolation
<b>Typed inheritance</b>	Not applicable	Meta-gated inter-array paths
<b>Cross-axis linkage</b>	Not applicable	Cross-reference registers
<b>Consistency checking</b>	Requires full inference + external logic	Read-before-write on same array
<b>Transitive classification</b>	Requires multi-layer + activation + softmax	Cascade reads within array
<b>Precision per junction</b>	4–8 bits (16–256 levels)	1.58 bits (3 levels)
<b>Read circuit</b>	Precision ADC	Two-threshold comparator
Three-valued logic	Not representable	Native
<b>For ICD-11 respiratory diseases</b>	~10M junctions (embeddings)	~136K junctions (assertions)
<b>Auditability</b>	Post-hoc explanation methods	Each junction’s address IS the evidence

numerical values to resistance states — the physical layout carries no algebraic meaning. HDC maps vector components to junctions — meaning is distributed. TCAM stores match patterns in flat arrays — entries can be rearranged arbitrarily. This work maps an entire algebra (Heyting lattice with typed Galois connections, established in Paper 2, together with cross-fiber bridges introduced in Paper 3) to a crossbar topology where the wiring IS the algebra. The specialization order is the chip’s inter-array connectivity. The meet is a topological common ancestor. The typing function, unfolded across inheritance edges, drives meta-controlled gates. Bridges across non-comparable fibers are cross-reference registers. The closure property is the physical idempotence of re-running inheritance. None of these structural correspondences exist in neural crossbars, HDC arrays, or TCAMs.

## 7.2. The Deeper Observation

Every computing architecture since von Neumann assumes that storage and computation require different physical mechanisms. Memory cells store; logic gates compute; buses connect them. Even "in-memory computing" only partially addresses this: memristive crossbars compute matrix products in memory, but interpretation, control flow, and decision logic remain external.

CDC’s domain algebra suggests why this separation persists: **prior data formats do not natively encode computational semantics**. A 16-bit floating-point weight of 0.7324 carries

no inherent semantic meaning — three identical weights in three different networks compute three different things. A ternary state of +1 at position (CA40.00, is\_a, Pneumonia) in the @Anatomical array carries the same meaning no matter what chip it is printed on. The position, the domain, the relation, and the ternary value together fix the semantics; no interpretive layer is needed.

When the data format is natively computational, the storage-computation separation dissolves — not just in theory (Paper 3), but in physics (this paper).

### 7.3. A Broader Structural Reading

The homomorphism  $\Phi$  admits a broader reading. The C-R@D-C' form is not unique to CDC: it appears in branching control flow (state  $\rightarrow$  transition@condition  $\rightarrow$  state), in abstract syntax trees, in state-transition machines, and in Kripke accessibility structures. Whether these constitute parallel instantiations of a common structural form, or merely share surface notation, is beyond the scope of this paper. We note only that the storage-computation dissolution demonstrated here in hardware is consistent with the software-layer result of Paper 3, suggesting the dissolution may not be substrate-specific. A characterization of what substrate properties suffice to support the C-R@D-C' form — and the conditions under which storage-computation separation reemerges — is left for future work.

### 7.4. Limitations

**Domain-specific.** This chip performs domain-constrained classification and reasoning. It does not do general-purpose computation, neural inference, or numerical simulation.

**Compile-time materialization.** The domain structure is fixed at fabrication. Runtime evolution of the domain lattice itself is not supported; software-level mechanisms that split or merge domains must generate a new materialization, which maps to a new chip (or a reconfigurable platform — not pursued here). For stable reference standards such as ICD-11 that update on yearly cycles, this boundary is acceptable; for fast-changing knowledge, it is a real limitation.

**Static knowledge within each materialization.** Reprogramming junctions requires write pulses. For rapidly changing assertions within a fixed domain structure, write endurance becomes relevant. A practical update protocol: freeze the chip during inference; batch-apply standard updates at fixed intervals; version the meta-array to roll back if inconsistency is detected.

**State drift.** RRAM and PCM devices exhibit resistance drift over months to years. A +1 junction drifting toward  $R_{\text{mid}}$  converts a clinical assertion to "undefined" rather than flipping it to the opposite truth value — as noted in §5.4, this is the safe failure direction for medical applications, since the system flags an unanswerable query rather than returning a silently incorrect one. Mitigation: periodic readout-and-refresh cycles; ECC across redundant fiber copies.

**Interconnect area overhead.** The claim that "the wiring is the algebra" commits the design to routing an irregular domain lattice directly onto 2D silicon metal layers. For the respiratory-chapter scale (47 arrays, tens of thousands of inter-array wires) this is tractable, but as the number of domains grows toward full ICD-11 (~500 domains) or beyond, irregular inter-array routing will dominate both floorplan area and critical-path delay — the dense 1T1R arrays become a small fraction of total silicon. Future scaled designs will likely need to map inter-array connections onto a programmable **Network-on-Chip (NoC)** fabric or a shared-bus arbitration layer with routing tables held in SRAM, trading pure topological mapping for spatial efficiency. The homomorphism  $\Phi$  would then hold up to a fixed routing indirection — a structurally unchanged but physically more realistic implementation.

**Proof-of-concept scale.** The design covers one ICD-11 chapter. Full deployment requires multi-chip integration or larger monolithic arrays, and — as above — likely a NoC-based inter-array fabric.

**No SPICE validation.** This paper provides a behavioral simulation (Section 5.4) but not transistor-level SPICE. The 10 ns cycle estimate is a timing budget, not a verified circuit simulation. Read-margin under process corners, sense-amplifier offset characterization, buffer-tree skew, and parasitic RC extraction on the inter-array wiring all remain to be characterized before tape-out.

## 8. Conclusion

We presented a memristive chip design grounded in a structural homomorphism  $\Phi$  between a materialized CDC domain algebra (Li, Wang & Zhao, 2026b) and a crossbar topology. The homomorphism preserves fiber isolation as array isolation, the specialization order as directed wiring, meet and Heyting implication as topological properties, ternary valuation as three resistance states, the typed Galois connection (after unfolding  $\tau$  over inheritance edges) as meta-controlled gates, cross-fiber bridges as cross-reference registers, and the closure property as physical idempotence.

This homomorphism is what separates the design from ternary memory. A TCAM stores values in a flat structure where physical layout is arbitrary. The CDC crossbar topology IS the domain algebra — the wiring encodes the specialization order, the gates encode the typing function, the registers encode the bridges, and rearranging connections changes reasoning semantics. **This is not a chip that stores medical knowledge. This is a chip whose physical structure is medical knowledge.**

Five reasoning capabilities — domain scoping, three-valued logic, transitive classification, typed inheritance, and write-time consistency checking — follow as direct consequences of the homomorphism, with cross-axis queries handled by bridge register lookups. Each is physically realized: array isolation prevents cross-domain leakage; three resistance states encode holds/negated/undefined; a row-column cascade circuit within each 1T1R array computes transitive closure; meta-gates control selective inheritance; read-before-write checks consistency; cross-reference registers implement bridges. Behavioral simulation at the nominal operating point ( $\sigma_{\log} = 0.15$ , SNR = 20 dB) observes zero errors across all six capabilities in 100,000 trials each, with a safety margin extending to  $\sigma_{\log} \approx 0.25$  before any errors appear — a margin that comfortably accommodates commercial RRAM device variability.

The fabrication requirements are modest: three resistance states per junction (vs. 16–256 for neural accelerators), 1T1R cells (standard), two-threshold comparators (vs. precision ADCs), a small SRAM bank for bridges, and ~136,000 memristive junctions for the respiratory chapter.

The broader implication: the storage-computation separation that has defined computing architecture since von Neumann persists because prior data formats do not carry algebraic structure. When the data representation has algebraic structure — as CDC’s domain Heyting algebra does — that structure can be materialized into physical topology at compile time, and the separation dissolves. In software (Paper 3) and in hardware (this paper).

One junction. One clinical assertion. One inference. No software.

## References

Borghetti, J., Snider, G. S., Kuekes, P. J., Yang, J. J., Stewart, D. R., & Williams, R. S. (2010). ‘Memristive’ switches enable ‘stateful’ logic operations via material implication. *Nature*, 464, 873–876.

- Chen, A., et al. (2015). *Emerging Nanoelectronic Devices*. Wiley.
- Hu, M., et al. (2018). Memristor-based analog computation and neural network classification with a dot product engine. *Advanced Materials*, 30(9), 1705914.
- Kanerva, P. (2009). Hyperdimensional computing: An introduction to computing in distributed representation with high-dimensional random vectors. *Cognitive Computation*, 1(2), 139–159.
- Karunaratne, G., Le Gallo, M., Cherubini, G., Benini, L., Rahimi, A., & Sebastian, A. (2020). In-memory hyperdimensional computing. *Nature Electronics*, 3(6), 327–337.
- Knuth, D. E. (1997). *The Art of Computer Programming, Volume 2: Seminumerical Algorithms* (3rd ed.). Addison-Wesley.
- Kvatinsky, S., Belousov, D., Liman, S., Satat, G., Wald, N., Friedman, E. G., Kolodny, A., & Weiser, U. C. (2014). MAGIC — Memristor-Aided Logic. *IEEE Transactions on Circuits and Systems II*, 61(11), 895–899.
- Li, C., Graves, C. E., Sheng, X., Miller, D., Foltin, M., Pedretti, G., & Strachan, J. P. (2020). Analog content-addressable memories with memristors. *Nature Communications*, 11, 1638.
- Li, C., Wang, Y., & Zhao, C. (2026a). Domain-constrained knowledge representation: A modal framework. arXiv:2604.01770.
- Li, C., Wang, Y., & Zhao, C. (2026b). Domain-contextualized inference: A computable graph architecture for explicit-domain reasoning. arXiv:2604.04344.
- Li, C., & Wang, Y. (2026c). Reasoning as data: Representation-computation unity and its implementation in a domain-algebraic inference engine. arXiv:2604.10908.
- Merolla, P. A., et al. (2014). A million spiking-neuron integrated circuit with a scalable communication network and interface. *Science*, 345(6197), 668–673.
- Pagiamtzis, K., & Sheikholeslami, A. (2006). Content-addressable memory (CAM) circuits and architectures: A tutorial and survey. *IEEE Journal of Solid-State Circuits*, 41(3), 712–727.
- Talati, N., Gupta, S., Mane, P., & Kvatinsky, S. (2016). Logic design within memristive memories using Memristor-Aided loGIC (MAGIC). *IEEE Transactions on Nanotechnology*, 15(4), 635–650.
- Wong, H.-S. P., & Salahuddin, S. (2015). Memory leads the way to better computing. *Nature Nanotechnology*, 10(3), 191–194.
- Wu, T. F., et al. (2021). Hyperdimensional computing exploiting carbon nanotube FETs, resistive RAM, and silicon CMOS to process a million-dimensional hypervectors. In *IEEE International Solid-State Circuits Conference (ISSCC)*.
- Yao, P., Wu, H., Gao, B., Tang, J., Zhang, Q., Zhang, W., Yang, J. J., & Qian, H. (2020). Fully hardware-implemented memristor convolutional neural network. *Nature*, 577(7792), 641–646.
- Yu, S., et al. (2011). A low energy oxide-based electronic synaptic device for neuromorphic visual systems with tolerance to device variation. *Advanced Materials*, 23(15), 1774–1779.
- The algebra is the topology. The topology is the chip. The chip is the reasoning.*